Magnetic Clusters

Polycationic Mn_{12} Single-Molecule Magnets as Electron Reservoirs with $S > 10$ Ground States[**]

Eugenio Coronado,[*] Alicia Forment-Aliaga, Alejandro Gaita-Ariño, Carlos Giménez-Saiz, Francisco M. Romero,[*] and Wolfgang Wernsdorfer

Magnetic clusters with a large-spin ground state and a significant magnetic anisotropy may develop a potential-

---

[*] Prof. E. Coronado, A. Forment-Aliaga, A. Gaita-Ariño,
Dr. C. Giménez-Saiz, Dr. F. M. Romero
Institut de Ciència Molecular
Universitat de València
Dr. Moliner 50, 46100 Burjassot (Spain)
Fax: (+34) 963-544-859
E-mail: eugenio.coronado@uv.es
fmrm@uv.es

Dr. W. Wernsdorfer
Laboratoire Louis Néel-CNRS
25, Avenue des Martyrs BP 166
38042 Grenoble Cedex 9 (France)

[**] This work was supported by the European Union (TMR HPRN-CT-1999-00012) and the Spanish Ministerio de Ciencia y Tecnología (MCT; Project No. MAT2001-5408-E). F.M.R. and C.G.S. thank the MCT for research contracts (Programa Ramón y Cajal). A.F.A. and A.G.A. thank, respectively, the Universitat de València and the Generalitat Valenciana for a predoctoral fellowship.

Supporting information for this article is available on the WWW under http://www.angewandte.org or from the author.

DOI: 10.1002/ange.200460282

energy barrier for reversal of the direction of magnetization. At low temperatures, the spin of a single cluster can be permanently magnetized in the direction of the applied field.[1] Switching off the field leads to typical magnetic relaxation phenomena and hysteresis loops are observed. Magnetic clusters of this kind are called single-molecule magnets (SMM). These systems provide a remarkable example of macroscopic quantum tunneling,[2] but their interest lies also in their possible application as nanomagnetic devices.

A well-known type of SMM is the family of dodecanuclear manganese complexes (Mn_{12}) of formula $[Mn_{12}O_{12}(O_2CR)_{16}(H_2O)_4]$.[3,4] These mixed-valence compounds contain four Mn^{IV} centers and eight Mn^{III} centers that are exchange-coupled to give a large-spin ground state ($S=10$). The axially distorted Mn^{III} centers provide the source for magnetic anisotropy and are also involved in the redox activity of the system. They can easily undergo reduction to Mn^{II}, so that the neutral Mn_{12} species can be transformed into the corresponding SMM Mn_{12}^{-} and Mn_{12}^{2-} ions with spin ground states $S=19/2$, 21/2 and $S=10$, respectively.[5,6] A modification of the magnetic behavior of the system is observed when these anions are combined with appropriate cations (paramagnetic and/or redox-active).[7,8] In this context, we have recently developed a strategy to synthesize and characterize polycationic Mn_{12} SMMs bearing 16 quaternary ammonium substituents in the periphery[9] by a carboxylate-exchange reaction between the acetate precursor $[Mn_{12}O_{12}(O_2CCH_3)_{16}(H_2O)_4]$ (Mn_{12}Ac) and tributylammonium salt $ZHPF_6$.

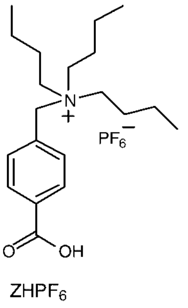
$ZHPF_6$

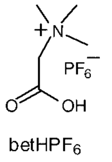
$betHPF_6$

The redox behavior of Mn_{12} derivatives is strongly correlated to the electron-withdrawing ability of the carboxylate ligands located in the periphery.[5b] A shorter separation between the cations and the $Mn_{12}O_{12}$ core should result in more stable reduced forms, as a result of the strong inductive effect caused by the cationic shell. We thus turned our attention to betaine hexafluorophosphate salt ($betHPF_6$) as the incoming carboxylic acid in the synthesis of $[Mn_{12}O_{12}(bet)_{16}(EtOH)_4](PF_6)_{14}\cdot 4\,CH_3CN\cdot H_2O$ (**1**), a two-electron reduced polycationic single-molecule magnet.

Complex **1** crystallizes in the centrosymmetric *P*2/*c* space group.[10]. The structure of the $Mn_{12}O_{12}$ core (Figure 1) is similar to that found in all Mn_{12} derivatives and comprises a central Mn_4O_4 cubane core surrounded by a nonplanar Mn_8O_8 ring held together with μ_3-oxo bridges. Peripheral bridging is ensured by sixteen η^2-μ-carboxylate anions which provide a positive charge of $z=+16$ per cluster. The high charge is partially compensated by the presence of 14 hexafluorophosphate anions in the crystal lattice. Electroneutrality can thus be achieved if the Mn_{12} molecules are considered as two-electron reduced species. Bond valence sum (BVS) calculations[11] (see Supporting Information) were performed to confirm this hypothesis. The structures of the central cubane units compare well with previous results and are characteristic of Mn^{IV} centers. Half of the manganese ions located in the Mn_8 rings (Mn3 and Mn5) are clearly Mn^{III} centers and exhibit Jahn–Teller distortion, with the anisotropy axes lying almost perpendicular to the mean plane of the cluster.[12] The four remaining coordination sites (Mn4, Mn6, and their symmetry equivalents) do not show axial distortion and exhibit longer Mn–O bonds, which indicates partial reduction to Mn^{II}. These four Mn atoms are in a +2.5 oxidation state according to BVS analysis. Interestingly, one of these Mn atoms (Mn6) is coordinated to two ethanol molecules located in axial positions. This arrangement yields four ethanol molecules per Mn_{12} species distributed in a "*trans*" (0:2:0:2) arrangement as a result of the local C_2 symmetry of the cluster. The polycations exhibit a propeller-like arrangement of the equatorial betaine ligands around the Mn_8 ring. All the magnetic clusters have the same orientation in the crystal lattice, with their symmetry axis situated parallel to the crystallographic *y* axis. Hexafluorophosphate anions and solvent molecules fill the intercluster space.

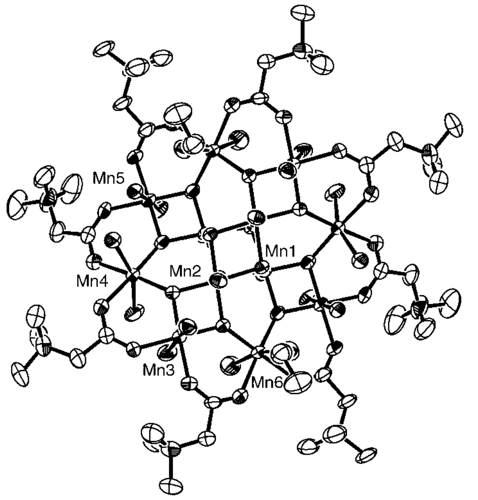

Figure 1. View along the *b* axis (ORTEP, ellipsoids are set at the 50% probability level) of the Mn_{12} polycation of **1** showing the propeller-like arrangement of the equatorial ligands (axial betaines and disordered EtOH molecules are omitted for clarity).

AC magnetic susceptibility measurements of **1** were performed at different frequencies on crystals dried under vacuum and dispersed in oil. Figure 2a shows the temperature dependence of $\chi'T$, where χ' is the real part of the AC molar magnetic susceptibility. The plateau observed in the 5–8 K range (68–69 emu K mol^{-1}) lies considerably above the typical values (45–50 emu K mol^{-1}) found for other Mn_{12} compounds and is close to the expected value for an $S=11$ ground state (66 emu K mol^{-1}). Frequency-dependent out-of-phase signals

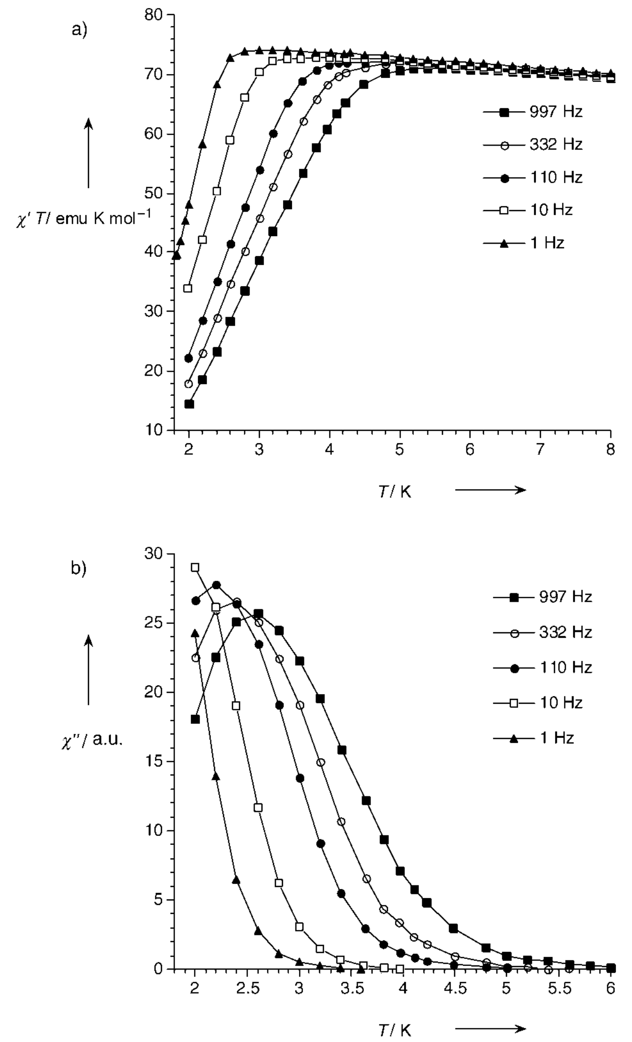

Figure 2. a) Thermal variation of the product of $\chi' T$ of **1** with temperature (in-phase component) at different frequencies. b) Temperature dependence of the out-of-phase χ'' component. a.u. = arbitray units.

with very broad maxima in the 2–4 K range were observed (see Supporting Information), which indicates partial desolvation of the sample. Measurements on wet samples (Figure 2b) afforded better results, and the presence of well-defined maxima in the 2–3 K range was confirmed. An effective energy barrier $U_{\mathrm{eff}} = 34$ K for reversal of the magnetization was determined from the frequency dependence of these maxima. The out-of-phase AC results are similar to those obtained for $(PPh_4)_2[Mn_{12}O_{12}(O_2CCHCl_2)_{16}(H_2O)_4]$ (**2**), the only two-electron reduced Mn_{12} species reported to date,[6b] and clearly support a reduced state for **1**. Upon reduction, some of the anisotropic Mn^{III} ions become Mn^{II}, and the intrinsic energy barrier for reversal of the spins is lowered compared to neutral Mn_{12} molecules. The $\chi''(T)$ maxima are then shifted to lower temperatures. A novel aspect of this work is that, whereas **2** seems to have the same $S = 10$ ground state as its neutral analogue, two-electron reduction results in a higher-spin ground state $S = 11$. This result is consistent with the usual spin topology of the cluster (spins of the Mn_4O_4 cubane core oriented antiparallel to the spins of the Mn_8 ring) determined by the strong Mn^{IV}–Mn^{III} antiferromagnetic coupling mediated by the double μ-oxo bridge.

To verify this hypothesis, DC magnetization data were collected at $H = 0.1$–5 T at different temperatures between 2 and 5 K (Figure 3). A spin Hamiltonian including a Zeeman term and axial and quartic zero-field splitting was used to fit the isofield data.[13] The value of the zero-field splitting parameter ($D = -0.22$ cm^{-1}), obtained by assuming an $S = 11$ ground state, compares well with the existing data for doubly reduced species.[6b] This value gives an activation energy $E = M_S^2 D = 38$ K, which is higher than the effective energy barrier obtained from the AC data ($U_{\mathrm{eff}} = 34$ K). This difference points to the presence of quantum tunneling through the barrier.

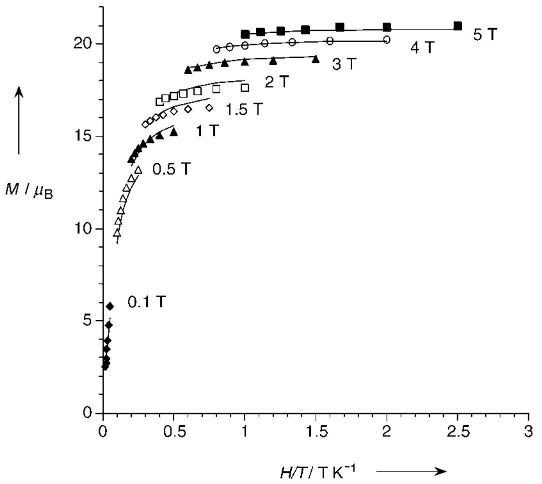

Figure 3. Plots of reduced magnetization M versus H/T for **1** at different field strengths H. The isofield lines are least-squares fits to the data according to ref. [13]. The best-fit values for the different parameters are $S = 11$, $g = 2.05$, $D = -0.22$ cm^{-1}, $B_4^0 = 0.41 \times 10^{-4}$ cm^{-1}.

Low-temperature magnetization measurements were performed on single crystals of **1** down to 0.04 K. The applied field was set parallel to the experimentally observed easy axis of magnetization. The SMM character of the sample was confirmed by the observation of hysteresis loops in the 1.6–0.25 K range that are strongly temperature dependent (Figure 4) and field sweep rate dependent (not shown). In contrast to the situation found in most Mn_{12} derivatives, hysteresis was only observed below 2 K, a fact that correlates with the decrease of the energy barrier that occurs upon reduction. The magnetization is saturated down to zero field, which indicates a well-defined spin ground state. Quantum tunneling of the magnetization is evidenced by the observation of temperature-independent loops below 0.25 K that remain strongly dependent on the field-sweep rate. Quantum steps are observed with regular spacings of 0.24 T magnetic field. This yields a $|D|$ parameter of 0.23 cm^{-1} that matches the value obtained from magnetization measurements. The smearing of the quantum steps at high temperatures and/or low magnetic fields can be interpreted in terms of a distribution of energy barriers. This has been confirmed by

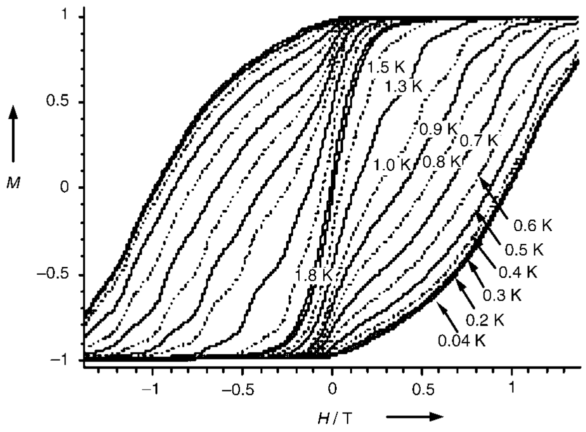

Figure 4. Single crystal measurement of magnetization *M* (normalized to its saturation value) versus field *H* applied in the direction of the easy axis of magnetization. The sweep rate was 0.035 $\mathrm{T\,s^{-1}}$.

relaxation measurements and is another indication of possible crystal defects subsequent to solvent losses.

The unusual oxidation state of this polycationic $\mathrm{Mn_{12}}$ compound is related to the strong electron-withdrawing ability of the trimethylammonium groups. Note that betaine hydrochloride has a very low pK_a value of 1.8, compared with the value for acetic acid (4.76). This electron-accepting character pushes the first and second reduction potentials of **1** to more positive values relative to most $\mathrm{Mn_{12}}$ compounds, as has been observed for the dichloroacetic acid derivative **2** with p$K_a = 1.29$. The differential pulse voltammogram (DPV) of **1** exhibits first and second reduction waves at $E = +0.49$ and $+0.21$ V (versus ferricinium/ferrocene couple), respectively. A third quasi-reversible reduction signal appears at -0.72 V (see Supporting Information). Thus, the stability range of the two-electron reduced species is extremely wide (ca. 1 V!) as compared with previous examples.

An interesting feature is that all of the reported syntheses of $\mathrm{Mn_{12}}$ reduced species employ iodide as reductant. It is possible that ethanol plays this role in the present example as manganese oxides are common reagents for the oxidation of alcohols.[14] Also, coordination of ethanol to the $\mathrm{Mn_{12}}$ core is unprecedented, and suggests further studies in which the nature of the ligands that occupy the four "water sites" is changed. Finally, preliminary results show that the polycationic compound **1** with an $S = 11$ ground state opens the way to the preparation of a variety of crystalline SMM salts by simple metathesis reactions, and that it is a useful precursor for the deposition of these magnetically active entities onto metal and metal oxide surfaces.

Experimental Section

All chemicals and solvents were used as received. $\mathrm{[Mn_{12}O_{12}(O_2CCH_3)_{16}(H_2O)_4]}$ ($\mathrm{Mn_{12}Ac_{16}}$) was prepared as previously described.[15]

betHPF$_6$: A solution of potassium hexafluorophosphate (5.4 g, 2.93 mmol) in hot water (33 mL) was slowly added to a stirred solution of betaine hydrochoride (4.5 g, 2.93 mmol) in hot water (18 mL). As the mixture cooled, betHPF$_6$ precipitated as a white crystalline powder. The product was filtered, washed with cold water, and dried under vacuum. Yield: 50%. ^{1}H NMR (300.1 MHz, $\mathrm{CD_3CN}$): $\delta = 3.95$ (s, 2H), 3.20 ppm (s, 9H); ^{13}C NMR (75.5 MHz, $\mathrm{CD_3CN}$): $\delta = 166.90$ (COOH), 64.84 ($\mathrm{CH_2}$), 54.53 ppm ($\mathrm{CH_3}$); IR (KBr): $\tilde{\nu} = 1739$ (s), 1479 (s), 1420 (m), 1266 (m), 1223 (m), 841 (s), 558 cm^{-1} (s); elemental analysis calcd (%) for $\mathrm{C_5H_{12}F_6NO_2P}$ (263.1): C 22.82, H 4.60, N 5.32; found: C 22.28, H 4.07, N 5.10.

1: $\mathrm{Mn_{12}Ac_{16}}$ (0.25 g, 0.125 mmol,) was added to a solution of betHPF$_6$ (0.60 g, 2.3 mmol) in $\mathrm{C_6H_5CN}$ (35 mL) and $\mathrm{CH_3CN}$ (20 mL). The mixture was stirred overnight, filtered, and the solvent was evaporated under reduced pressure to complete precipitation. The solid was collected by filtration and dissolved in a small amount of $\mathrm{CH_3CN}$. After addition of toluene, the solution was evaporated to dryness to remove the acetic acid as the toluene azeotrope. This stage was repeated twice. The product was then dissolved in $\mathrm{C_6H_5CN}$ (35 mL) and $\mathrm{CH_3CN}$ (20 mL) and treated again with excess betHPF$_6$. The entire process was repeated. Finally, the product was dissolved in $\mathrm{CH_3CN}$ (35 mL). The resulting solution was then filtered and layered with EtOH. Black plates suitable for X-ray crystallography formed after a few days at room temperature. ^{1}H NMR (300.1 MHz, $\mathrm{CD_3CN}$): $\delta = 42$–39 ($\mathrm{CH_2}$), 39–33 ($\mathrm{CH_2}$), 30–25 ($\mathrm{CH_2}$), 16.9–15.5 ($\mathrm{CH_2}$), 15.5–14.2 ($\mathrm{CH_2}$), 6.3–4.6 ($\mathrm{CH_3}$), 4.0 ($\mathrm{CH_3}$), 3.01 ($\mathrm{CH_3}$), 2.12 ($\mathrm{CH_3}$), 2.03 ($\mathrm{CH_3}$), 0.80 ppm ($\mathrm{CH_3}$); ^{19}F NMR (282.4 MHz, $\mathrm{CD_3CN}$): $\delta = 68.52$ ppm (d, $J_{\mathrm{F,P}} = 709$ Hz); ^{31}P NMR (121.5 MHz, $\mathrm{CD_3CN}$): $\delta = -142.20$ ppm (m, $J_{\mathrm{P,F}} = 709$ Hz); IR (KBr): $\tilde{\nu} = 3065$ (w), 2967 (w), 1626 (s), 1495 (w), 1436 (m), 1410 (m), 1341 (m), 1240 (w), 967 (w), 910 (w), 837 (s), 725 (w), 619 (w), 558 (m), 461 cm^{-1} (w); ESI-MS ($\mathrm{CH_3CN}$, 30 V): m/z: 2159 $\{[\mathrm{Mn_{12}O_{12}(bet)_{16}](PF_6)_{11} + 1\,e^{-1}}\}^{2+}$; 2086 $\{[\mathrm{Mn_{12}O_{12}(bet)_{16}](PF_6)_{10} + 2\,e^{-1}}\}^{2+}$; 2028 $\{[\mathrm{Mn_{12}O_{12}(bet)_{15}]\text{-}(PF_6)_{10} + 2\,e^{-1}}\}^{2+}$; 1956 $\{[\mathrm{Mn_{12}O_{12}(bet)_{15}](PF_6)_9 + 3\,e^{-1}}\}^{2+}$; 1007 $\{[\mathrm{Mn_{12}O_{12}(bet)_{16}](PF_6)_9 + 1\,e^{-1}}\}^{4+}$, 777 $\{[\mathrm{Mn_{12}O_{12}(bet)_{16}](PF_6)_8 + 1\,e^{-1}}\}^{5+}$; elemental analysis calcd (%) for $[\mathrm{Mn_{12}O_{12}(bet)_{16}](PF_6)_{14}}$ (4755.1): C 20.21, H 3.73, N 4.71; found: C 19.86, H 4.26, N 4.46.

Physical measurements: NMR spectra were recorded on a Bruker Avance DRX 300-MHz spectrometer. ESI mass spectra were recorded on a Waters ZQ mass spectrometer using nitrogen as the drying and nebulizing gas. The equipment was calibrated with appropriate standard samples. All the magnetic measurements were carried out on polycrystalline samples with a magnetometer (Quantum Design MPMS-XL-5) equipped with a SQUID sensor. The samples were dispersed in oil to avoid torquing of the crystals. Variable-temperature susceptibility measurements were carried out at 2–300 K in a 0.1 T magnetic field. The susceptibility data were corrected for the diamagnetic contributions of the salts, as deduced by using a Pascal constants table. The AC measurements were performed in the temperature range 2–8 K at different frequencies with an oscillating magnetic field of $H = 0.395$ mT. The magnetization data were collected in the $H = 0$–5 T field range at different temperatures between 2 and 5 K. The hysteresis studies were performed at $T = 2$ K with H between 5 and −5 T, at, with sample cooling at zero field. Low-temperature magnetization measurements were performed on single crystals of **1** at 0.04–7 K using a micro-SQUID apparatus at different sweep rates between 0.1 and 0.001 $\mathrm{T\,s^{-1}}$.[16] The applied field was parallel to the experimentally observed easy axis of magnetization. IR transmission measurements of pressed KBr pellets were recorded at room temperature with a Nicolet Avatar 320 FTIR spectrophotometer ($\tilde{\nu} = 4000$–400 cm^{-1}). C,H,N elemental analysis was carried out on samples dried under vacuum in a CE instruments EA 1110 CHNS analyzer.

Received: April 9, 2004
Revised: July 21, 2004

Keywords: carboxylate ligands · magnetic properties · manganese · mixed-valent compounds · single-molecule studies

[1] R. Sessoli, D. Gatteschi, A. Caneschi, M. A. Novak, *Nature* **1993**, *365*, 141.

[2] a) J. Friedman, M. Sarachik, J. Tejada, R. Ziolo, *Phys. Rev. Lett.* **1996**, *76*, 3830; b) J. Hernández, X. Zhang, F. Louis, J. Bartolomé, J. Tejada, R. Ziolo, *Europhys. Lett.* **1996**, *35*, 301; c) L. Thomas, F. Lionti, R. Ballou, D. Gatteschi, R. Sessoli, B. Barbara, *Nature* **1996**, *383*, 145.

[3] a) A. Caneschi, D. Gatteschi, R. Sessoli, A. L. Barra, L. C. Brunel, M. Guillot, *J. Am. Chem. Soc.* **1991**, *113*, 5873; b) R. Sessoli, H.-L. Tsai, A. R. Schake, S. Wang, J. B. Vincent, K. Folting, D. Gatteschi, G. Christou, D. N. Hendrickson, *J. Am. Chem. Soc.* **1993**, *115*, 1804; c) G. Christou, D. Gatteschi, D. N. Hendrickson, R. Sessoli, *Mater. Res. Bull.* **2000**, *35*, 66.

[4] D. Gatteschi, A. Caneschi, L. Pardi, R. Sessoli, *Science* **1994**, *265*, 1054.

[5] a) A. R. Schake, H.-L. Tsai, N. de Vries, R. J. Webb, K. Folting, D. N. Hendrickson, G. Christou, *J. Chem. Soc. Chem. Commun.* **1992**, 181; b) H. J. Eppley, H.-L. Tsai, N. de Vries, K. Folting, G. Christou, D. N. Hendrickson, *J. Am. Chem. Soc.* **1995**, *117*, 301; c) S. M. J. Aubin, Z. Sun, L. Pardi, J. Krzystek, K. Folting, L. C. Brunel, A. L. Rheingold, G. Christou, D. N. Hendrickson, *Inorg. Chem.* **1999**, *38*, 5329.

[6] a) M. Soler, S. K. Chandra, D. Ruiz, E. R. Davidson, D. N. Hendrickson, G. Christou, *Chem. Commun.* **2000**, 2417; b) M. Soler, W. Wernsdorfer, K. A. Abboud, J. C. Huffman, E. R. Davidson, D. N. Hendrickson, G. Christou, *J. Am. Chem. Soc.* **2003**, *125*, 3576.

[7] K. Takeda, K. Awaga, *Phys. Rev. B* **1997**, *56*, 14560.

[8] T. Kuroda-Sowa, M. Lam, A. L. Rheingold, C. Frommen, W. M. Reiff, M. Nakano, J. Yoo, A. L. Maniero, L. C. Brunel, G. Christou, D. N. Hendrickson, *Inorg. Chem.* **2001**, *40*, 6469.

[9] a) E. Coronado, M. Feliz, A. Forment-Aliaga, C. J. Gómez-García, R. Llusar, F. M. Romero, *Inorg. Chem.* **2001**, *40*, 6084; b) A. Forment-Aliaga, E. Coronado, M. Feliz, A. Gaita-Ariño, R. Llusar, F. M. Romero, *Inorg. Chem.* **2003**, *42*, 8019.

[10] Crystal data for **1**: $C_{96}H_{214}F_{84}Mn_{12}N_{20}O_{49}P_{14}$, $M_r = 5121.73$, monoclinic, space group $P2/c$, $a = 20.7870(4)$, $b = 18.3190(4)$, $c = 31.1280(7)$ Å, $\beta = 117.0730(10)°$, $V = 10554.6(4)$ Å^3, $Z = 2$, $\rho_{calcd} = 1.612$ Mg m^{-3}, $\mu(Mo_{K\alpha}) = 0.939$ mm^{-1}. A dark brown platelike single crystal of **1** of dimensions $0.25 \times 0.10 \times 0.04$ mm^3 was used for data collection on a Nonius Kappa CCD diffractometer ($3.54° < 2\theta < 50.74°$) equipped with a graphite monochromated $Mo_{K\alpha}$ radiation source ($\lambda = 0.71073$ Å). Data collection was performed at 180(2) K. Of 112612 measured reflections, 19136 were independent ($R_{int} = 0.0868$) and used to refine 1278 parameters and 89 restraints. A multiscan absorption correction, based on equivalent reflections, was applied to the data using the program SORTAV[17] ($T_{max}/T_{min} = 0.9626/0.7613$). The structure was solved by direct methods (SIR97)[18] and refined against F^2 with a full-matrix least-squares algorithm using SHELX-97[19] and the WinGX (1.64) software package.[20] One ethanol molecule shows orientational disorder that was modeled with a set of two positions for each carbon atom having refined occupancies close to 0.5. These occupancies were fixed to 0.5 in the last cycles of refinement and refined isotropically. The disordered C atoms were presumed to have the same isotropic displacement parameters. Furthermore, C–C and C–O distances were restrained so that they were the same for both orientations within the same molecule. This kind of disorder in the coordinated ethanol molecule has also been observed in several Mn^{III}–Schiff base complexes.[21] A water molecule with an occupancy of 0.5 was located near this disordered ethanol molecule. The other ethanol molecule coordinated to Mn6 is not disordered and was refined anisotropically. Nine different hexafluorophosphate anions were located, three of them on special positions and one (on a general position) with a refined occupancy of 0.5, thus accounting for the +14 charge of the Mn_{12} complex. Four acetonitrile solvent molecules were also located, which had refined occupancies of 0.5 that were fixed to this value in the last cycles of refinement. Geometrical restraints were applied to some of the hexafluorophosphate anions and solvent molecules which had high anisotropic displacement parameters. All the remaining non-hydrogen atoms were refined anisotropically. The positions of the H atoms on the C atoms were added into the calculated positions and refined on the corresponding atoms. H atoms on the O atoms of ethanol molecules were refined using the AFIX 147 instruction of SHELX-97. The H atoms of the water molecule were placed in theoretical positions using Nardelli's method. These H atoms were included in structure-factor calculations with fixed positional parameters and isotropic displacement parameters of 0.05 Å^2. Final R ($I > 2\sigma(I)$), $R_1 = 0.0853$, $wR_2 = 0.2284$; final R (all data), $R_1 = 0.1304$, $wR_2 = 0.2723$. Max./min. residual electron density 1.135/−1.378 e Å^{-3}. CCDC-235825 contains the supplementary crystallographic data for this paper. These data can be obtained free of charge via www.ccdc.cam.ac.uk/conts/retrieving.html (or from the Cambridge Crystallographic Data Centre, 12 Union Road, Cambridge CB21EZ, UK; fax: (+44)1223-336-033; or deposit@ccdc.cam.ac.uk).

[11] I. D. Brown, D. Altermatt, *Acta Crystallogr. Sect. B* **1985**, *41*, 244.

[12] S. M. J. Aubin, Z. Sun, H. J. Eppley, E. M. Rumberger, I. A. Guzei, K. Folting, P. K. Gantzel, A. L. Rheingold, G. Christou, D. N. Hendrickson, *Inorg. Chem.* **2001**, *40*, 2127.

[13] The complete spin Hamiltonian is given by the following expression:[22]
$\hat{\mathbf{H}} = -g\mu_B H\hat{\mathbf{S}} + D[\hat{S}_z^2 - {}^1\!/_3 S(S+1)] + B_4^0\hat{\mathbf{O}}_4^0$.
The best-fit values for the different parameters are $g = 2.05$, $D = -0.22$ cm^{-1}, $B_4^0 = 0.41 \times 10^{-4}$ cm^{-1}. The g value obtained is slightly higher than expected for a Mn_{12} cluster ($g < 2$). A scaling factor of 3% can solve this problem, which lies within experimental uncertainty.

[14] E. P. Papadopoulos, A. Jarrar, C. H. Issidorides, *J. Org. Chem.* **1966**, *31*, 615.

[15] T. Lis, *Acta Crystallogr. Sect. B* **1980**, *36*, 2042.

[16] W. Wernsdorfer, *Adv. Chem. Phys.* **2001**, *118*, 99.

[17] R. H. Blessing, *J. Appl. Crystallogr.* **1997**, *30*, 421.

[18] A. Altomare, M. C. Burla, M. Camalli, G. Cascarano, C. Giacovazzo, A. Guagliardi, A. G. G. Moliterni, G. Polidori, R. Spagna, *J. Appl. Crystallogr.* **1999**, *32*, 115.

[19] G. M. Sheldrick, SHELX-97, an integrated system for solving and refining crystal structures from diffraction data, University of Göttingen, Germany, **1997**.

[20] L. J. Farrugia, *J. Appl. Crystallogr.* **1999**, *32*, 837.

[21] I. V. Korendovych, E. V. Rybak-Akimova, *Acta Crystallogr. Sect. C* **2004**, *60*, m82.

[22] P. Artus, C. Boskovic, J. Yoo, W. E. Streib, L. C. Brunel, D. N. Hendrickson, G. Christou, *Inorg. Chem.* **2001**, *40*, 4199.